We are IntechOpen,
the world's leading publisher of
Open Access books
Built by scientists, for scientists

6,900
Open access books available

186,000
International authors and editors

200M
Downloads

Our authors are among the

154
Countries delivered to

TOP 1%
most cited scientists

12.2%
Contributors from top 500 universities

CLARIVATE ANALYTICS
BOOK CITATION INDEX
INDEXED

WEB OF SCIENCE™

Selection of our books indexed in the Book Citation Index
in Web of Science™ Core Collection (BKCI)

Interested in publishing with us?
Contact book.department@intechopen.com

Numbers displayed above are based on latest data collected.
For more information visit www.intechopen.com

Assessment of Various Methods in Solving Inverse Heat Conduction Problems

M. S. Gadala and S. Vakili
Department of Mechanical Engineering, The University of British Columbia,
Vancouver, BC,
Canada

1. Introduction

In an inverse heat conduction problem (IHCP), the boundary conditions, initial conditions, or thermo-physical properties of material are not fully specified, and they are determined from measured internal temperature profiles. The challenge is that the effect of changes in boundary conditions are normally damped or lagged, i.e. the varying magnitude of the interior temperature profile lags behind the changes in boundary conditions and is generally of lesser magnitude. Therefore, such a problem would be a typically ill-posed and would normally be sensitive to the measurement errors. Also, in the uniqueness and stability of the solution are not generally guaranteed (Beck et al., 1985; Alifanov, 1995; Ozisik, 2000).

Inverse heat conduction problems, like most of the inverse problems encountered in science and engineering may be reformulated as an optimization problem. Therefore, many available techniques of solving the optimization problems are available as methods of solving the IHCPs. However, the corresponding objective function of the inverse problems can be highly nonlinear or non-monotonic, may have a very complex form, or in many practical applications, its analytical expression may be unknown. The objective function usually involves the squared difference between measured and estimated unknown variables. If $\mathbf{Y}$ and $\mathbf{T}$ are the vectors of the measured and estimated temperatures, then the objective function will be in the form of

$$U = [\mathbf{Y} - \mathbf{T}]^{\mathrm{T}}[\mathbf{Y} - \mathbf{T}] \tag{1}$$

However, normally there is need for another term, called "regularization" in order to eliminate the oscillations in the results and make the solution more stable. The effect of this term and the strategy of choosing it will be discussed in details in the subsequent chapters.

The above equation is only valid, if the measured temperatures and the associated errors have the following statistical characteristics (Beck & Arnold, 1977):

- The errors are additive, i.e.

$$Y_i = T_i + \varepsilon_i \tag{2}$$

where ε_i is the random error associated with the ith measurement.

- The temperature errors have zero mean.
- The errors have constant variance.

- The errors associated with different measurements are uncorrelated.
- The measurement errors have a normal (Gaussian) distribution.
- The statistical parameters describing the errors, such as their variance, are known.
- Measured temperatures are the only variables that contain measurement errors. Measured time, positions, dimensions, and all other quantities are all accurately known.
- There is no more prior information regarding the quantities to be estimated. If such information is available, it should be utilized to improve the estimates.

While classical methods, such as the least square regularization method (Beck et al., 1985; Beck et al., 1996), the sequential function specification method (Alifanov, 1995; Beck et al., 1996; Blanc et al., 1998), the space marching method (Al-Khalidy, 1998), conjugate gradient method (Abou khachfe & Jarny, 2001; Huang & Wang, 1999), steepest descent method (Huang et al., 2003), and the model reduction algorithm (Battaglia, 2002; Girault et al., 2003) are vastly studied in the literature, and applied to the problems in thermal engineering (Bass, 1980; Osman, 1190; Kumagai et al., 1995; Louahia-Gualous et al., 2003; Kim & Oh, 2001; Pietrzyk & Lenard, 1990; Alifanov et al., 2004; Gadala & Xu, 2006), there are still some unsolved problems:

- The solution often shows some kinds of overshoot and undershoot, which may result in non-physical answers.
- Very high heat flux peak values such as those experienced in jet impingement cooling are normally damped and considerably underestimated.
- Results are very sensitive to the quality of input. Measurement errors are intrinsic in laboratory experiments, so we need a more robust approach in solving the inverse problem.
- The time step size that can be used with these methods is bounded from below, and cannot be less than a specific limit (Beck et al., 1985). This causes temporal resolutions that are not sufficient for some real world applications, where changes happen very fast.

More recent optimization techniques may be used in the solution of the IHCPs to aid in stability, solution time, and to help in achieving global minimum solutions. Some of these techniques are briefly reviewed in the following section:

Genetic algorithm

This technique has been widely adopted to solve inverse problems (Raudensky et al., 1995; Silieti et al., 2005; Karr et al., 2000). Genetic algorithms (GAs) belong to the family of computational techniques originally inspired by the living nature. They perform random search optimization algorithms to find the global optimum to a given problem. The main advantage of GAs may not necessarily be their computational efficiency, but their robustness, i.e. the search process may take much longer than the conventional gradient-based algorithms, but the resulting solution is usually the global optimum. Also, they can converge to the solution when other classical methods become unstable or diverge. However, this process can be time consuming since it needs to search through a large tree of possible solutions. Luckily, they are inherently parallel algorithms, and can be easily implemented on parallel structures.

Neural networks

Artificial neural networks can be successfully applied in the solution of inverse heat conduction problems (Krejsa et al., 1999; Shiguemori et al., 2004; Lecoeuche et al., 2006).

They are capable of dealing with significant non-linearities and are known to be effective in damping the measurement errors.

Self-learning finite elements

This methodology combines neural network with a nonlinear finite element program in an algorithm which uses very basic conductivity measurements to produce a constitutive model of the material under study. Through manipulating a series of neural network embedded finite element analyses, an accurate constitutive model for a highly nonlinear material can be evolved (Aquino & Brigham, 2006; Roudbari, 2006). It is also shown to exhibit a great stability when dealing with noisy data.

Maximum entropy method

This method seeks the solution that maximizes the entropy functional under given temperature measurements. It converts the inverse problem to a non-linear constrained optimization problem. The constraint is the statistical consistency between the measured and estimated temperatures. It can guarantee the uniqueness of the solution. When there is no error in the measurements, maximum entropy method can find a solution with no deterministic error (Kim & Lee, 2002).

Proper orthogonal decomposition

Here, the idea is to expand the direct problem solution into a sequence of orthonormal basis vectors, describing the most essential features of spatial and temporal variation of the temperature field. This can result in the filtration of the noise in the field under study (Ostrowski et al., 2007).

Particle Swarm Optimization (PSO)

This is a population based stochastic optimization technique, inspired by social behavior of bird flocking or fish schooling. Like GA, the system is initialized with a population of random solutions and searches for optima by updating generations. However, unlike GA, PSO has no evolution operators such as crossover and mutation. In PSO, the potential solutions, called particles, fly through the problem space by following the current optimum particles. Compared to GA, the advantages of PSO are the ease of implementation and that there are few parameters to adjust. Some researchers showed that it requires less computational expense when compared to GA for the same level of accuracy in finding the global minimum (Hassan et al., 2005).

In this chapter, in addition to the classical function specification method, we will study the genetic algorithm, neural network, and particle swarm optimization techniques in more details. We will investigate their strengths and weaknesses, and try to modify them in order to increase their efficiency and effectiveness in solving inverse heat conduction problems.

2. Function specification methods

As mentioned above, in order to stabilize the solution to the ill-posed IHCP, it is very common to include more variables in the objective function. A common choice in inverse heat transfer problems is to use a scalar quantity based on the boundary heat fluxes, with a weighting parameter a, which is normally called the regularization parameter. The regularization term can be linked to the values of heat flux, or their first or second

derivatives, with respect to time or space. Previous research (Gadala & Xu, 2006) has shown that using the heat flux values (zeroth-order regularization) is the most suitable choice. The objective function then will be

$$F(\mathbf{q}) = \sum_{i=1}^{N} (\mathbf{T}_m^i - \mathbf{T}_c^i)^T (\mathbf{T}_m^i - \mathbf{T}_c^i) + \alpha \sum_{i=1}^{N} \mathbf{q}^{iT} \mathbf{q}^i \qquad (3)$$

where $\mathbf{T_m^i}$ and $\mathbf{T_c^i}$ are the vectors of expected (measured) and calculated temperatures at the ith time step, respectively, each having J spatial components; a is the regularization coefficient; and q^i is the boundary heat flux. It is important to notice that in the inverse analysis, the number of spatial components is equal in the measured and calculated temperature vectors; i.e. the spatial resolution of the recovered boundary heat flux vector is determined by the number of embedded thermocouples.

Due to the fact that inverse problems are generally ill-posed, the solution may not be unique and would be in general sensitive to measurement errors. To decrease such sensitivity and improve the simulation, a number of future time steps (n_{FTS}) are utilized in the analysis of each time step. This means that in addition to the measured temperature at the present time step T^i, the measured temperatures at future time steps, $T^{i+1}, T^{i+2}, ..., T^{i+n_{FTS}}$, are also used to approximate the heat flux q^i. In this process, a temporary assumption would be usually considered for the values of $q^{i+1}, q^{i+2}, ..., q^{i+n_{FTS}}$. The simplest and the most widely used one is to assume $q^{i+k} = q^i$ for $1 \le k \le n_{FTS}$, which is also used in our work. In this chapter, a combined function specification-regularization method is used, which utilizes both concepts of regularization, and future time steps (Beck & Murio, 1986).

Mathematically we may express T_c^k, the temperature at the kth time step and at location c as an implicit function of the heat flux history and initial temperature:

$$\mathrm{T}_c^k = f(\mathrm{q}^1, \mathrm{q}^2, ..., \mathrm{q}^k, T_c^0) \qquad (4)$$

and the following equation is valid

$$\mathrm{T}_c^k = \mathrm{T}_c^{k*} + \frac{\partial \mathrm{T}_c^1}{\partial \mathrm{q}^1}(\mathrm{q}^1 - \mathrm{q}^{1*}) + \frac{\partial \mathrm{T}_c^2}{\partial \mathrm{q}^2}(\mathrm{q}^2 - \mathrm{q}^{2*}) + ... + \frac{\partial \mathrm{T}_c^k}{\partial \mathrm{q}^k}(\mathrm{q}^k - \mathrm{q}^{k*}) \qquad (5)$$

The values with a '*' superscript in the above may be considered as initial guess values.

The first derivative of temperature $\mathbf{T}_c^i$ with respect to heat flux q^i is called the sensitivity matrix:

$$\mathbf{X}^i = \frac{\partial \mathbf{T}_c^i}{\partial \mathbf{q}^i} = \begin{bmatrix} a_{11}(i) & a_{12}(i) & ... & a_{1J}(i) \\ a_{21}(i) & a_{22}(i) & ... & a_{2J}(i) \\ \vdots & \vdots & \ddots & \vdots \\ a_{L1}(i) & a_{L2}(i) & ... & a_{LJ}(i) \end{bmatrix} \qquad (6)$$

$$a_{rs}(i) = \frac{\partial T_{cr}^i}{\partial q_s^i} \qquad (7)$$

The optimal solution for Eq. (3) may be obtained by setting $\partial F / \partial \mathbf{q} = 0$, which results in the following set of equations (note that $\partial F / \partial \mathbf{q}$ should be calculated with respect to each component q^i, with i=1, 2…N):

$$\left\{ \sum_{i=1}^{N} \left(\frac{\partial \mathbf{T}_c^i}{\partial \mathbf{q}^j} \right)_{\mathbf{q}^j = \mathbf{q}^{j*}}^{T} \left(\frac{\partial \mathbf{T}_c^i}{\partial \mathbf{q}^j} \right)_{\mathbf{q}^j = \mathbf{q}^{j*}} + \alpha \, \mathbf{I} \right\} (\mathbf{q}^j - \mathbf{q}^{j*}) =$$
$$\sum_{i=1}^{N} \left(\frac{\partial T_c^i}{\partial \mathbf{q}^j} \right)_{\mathbf{q}^j = \mathbf{q}^{j*}}^{T} \left(\mathbf{T}_m^i - \mathbf{T}_c^{i*} \right) - \alpha \, \mathbf{q}^{j*} \tag{8}$$
$$j = 1, 2, \ldots, N$$

where $\mathbf{q}^{j*}$ is the initial guess of heat fluxes, $\mathbf{T}_c^{i*}$ is the calculated temperature vector with the initial guess values.

Recalling equations (6) and (7), equation (8) may be rearranged and written in the following form:

$$(\mathbf{X}_{\mathbf{q}=\mathbf{q}^*}^{T} \mathbf{X}_{\mathbf{q}=\mathbf{q}^*} + \alpha \, \mathbf{I})(\mathbf{q} - \mathbf{q}^*) = \mathbf{X}^T \Delta \mathbf{T} - \alpha \, \mathbf{q}^* \tag{9}$$

where $\mathbf{X}$ is the total sensitivity matrix for multi-dimensional problem and has the following form:

$$\mathbf{X} = \begin{bmatrix} \mathbf{X}^1 & 0 & 0 & 0 \\ \mathbf{X}^2 & \mathbf{X}^1 & 0 & 0 \\ \vdots & \vdots & \ddots & 0 \\ \mathbf{X}^N & \ldots & \mathbf{X}^2 & \mathbf{X}^1 \end{bmatrix} \tag{10}$$

and

$$\Delta \mathbf{T} = \left(\mathbf{T}_m^1 - \mathbf{T}_c^{1*} \quad \mathbf{T}_m^2 - \mathbf{T}_c^{2*} \quad \ldots \quad \mathbf{T}_m^N - \mathbf{T}_c^{N*} \right)^T \tag{11}$$

By solving Eq. (9), the heat flux update will be calculated and added to the initial guess. In this chapter, a fully sequential approach with function specification is used. First, the newly calculated $\mathbf{q}^{1^n}$ is used for all time steps in the computation window after the first iteration, i.e., constant function specification is used for this computation window. Then, the computation window moves one time step at the next sequence after obtaining a convergent solution in the current sequence.

One important consideration in calculating the sensitivity values is the nonlinearity. The whole sensitivity matrix is independent of the heat flux only if the thermal properties of the material are not changing with temperature. For most materials, the thermophysical properties are temperature dependent. In such case, all properties should be updated at the beginning of each time step, which is time consuming especially for large size models. Moreover, such changes in properties would not be very large and would not significantly change the magnitude of the sensitivity coefficients. Also, updating the material properties at the beginning of each time step would be based on the temperatures $\mathbf{T}^{k*}$ obtained from the initially given values of heat flux $\mathbf{q}^*$, which is essentially an approximation. So, we may

update the sensitivity matrix every M steps (in our numerical experiments, M=10). The results obtained under this assumption were very close to those obtained by updating the values at each step, so the assumption is justified.

To obtain an appropriate level of regularization, the number of future time steps (or more accurately, the size of look-ahead time window, i.e. the product of the number of future time steps and time step size) and the value of the regularization parameter must be chosen with respect to the errors involved in the temperature readings. The residual principle (Alifanov, 1995; Woodbury & Thakur, 1996) has been used to determine these parameters based on the accuracy of thermocouples in the relative temperature range.

3. Genetic algorithm

Genetic algorithm is probably the most popular stochastic optimization method. It is also widely used in many heat transfer applications, including inverse heat transfer analysis (Gosselin et al., 2009). Figure 1 shows a flowchart of the basic GA. GA starts its search from a randomly generated population. This population evolves over successive generations (iterations) by applying three major operations. The first operation is "Selection", which mimics the principle of "Survival of the Fittest" in nature. It finds the members of the population with the best performance, and assigns them to generate the new members for future generations. This is basically a sort procedure based on the obtained values of the objective function. The number of elite members that are chosen to be the parents of the next generation is also an important parameter. Usually, a small fraction of the less fit solutions are also included in the selection, to increase the global capability of the search, and prevent a premature convergence. The second operator is called "Reproduction" or "Crossover", which imitates mating and reproduction in biological populations. It propagates the good features of the parent generation into the offspring population. In numerical applications, this can be done in several ways. One way is to have each part of the array come from one parent. This is normally used in binary encoded algorithms. Another method that is more popular in real encoded algorithms is to use a weighted average of the parents to produce the children. The latter approach is used in this chapter. The last operator is "Mutation", which allows for global search of the best features, by applying random changes in random members of the generation. This operation is crucial in avoiding the local minima traps. More details about the genetic algorithm may be found in (Davis, 1991; Goldberg, 1989).

Among the many variations of GAs, in this study, we use a real encoded GA with roulette selection, intermediate crossover, and uniform high-rate mutation (Davis, 1991). The crossover probability is 0.2, and the probability of adjustment mutation is 0.9. These settings were found to be the most effective based on our experience with this problem. A mutation rate of 0.9 may seem higher than normal. This is because we start the process with a random initial guess, which needs a higher global search capability. However, if smarter initial guesses are utilized, a lower rate of mutation may be more effective. Genes in the present application of GA consist of arrays of real numbers, with each number representing the value of the heat flux at a certain time step, or a spatial location.

4. Particle Swarm Optimization

We start by giving a description of the basic concepts of the algorithm. Then a brief description of the three variations of the PSO algorithm that are used in this study is given.

Finally we investigate some modifications in PSO algorithm to make it a more robust and efficient solver for the inverse heat conduction problem.
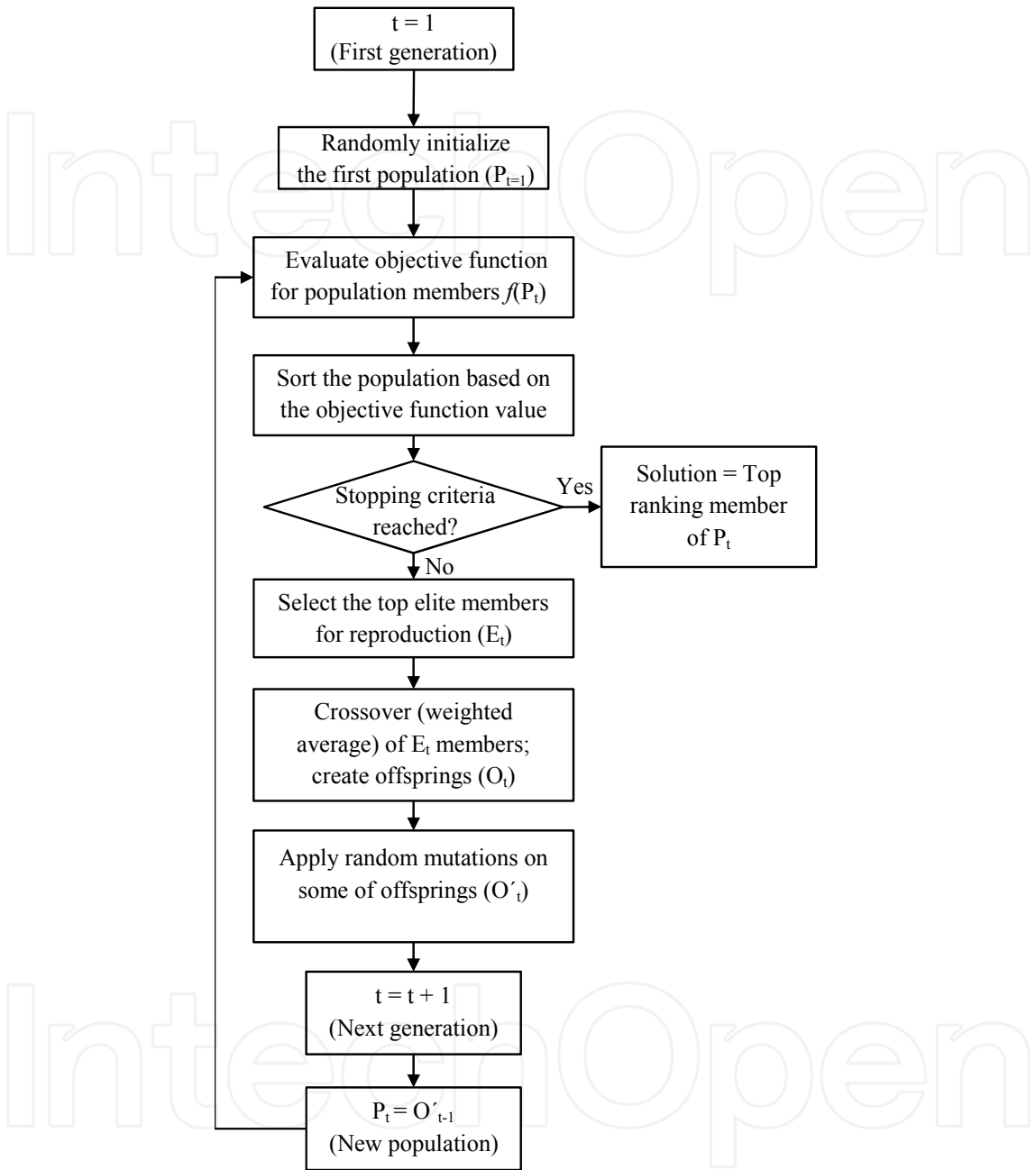
```
         ┌─────────────────┐
         │     t = 1       │
         │ (First generation)│
         └─────────────────┘
                  │
                  ▼
         ┌─────────────────┐
         │ Randomly initialize│
         │ the first population (P_{t=1})│
         └─────────────────┘
                  │
                  ▼
    ┌───►┌─────────────────────┐
    │    │ Evaluate objective function│
    │    │ for population members f(P_t)│
    │    └─────────────────────┘
    │              │
    │              ▼
    │    ┌─────────────────────┐
    │    │ Sort the population based on│
    │    │ the objective function value│
    │    └─────────────────────┘
    │              │
    │              ▼
    │          ◇ Stopping criteria ◇──Yes──► ┌──────────────┐
    │            reached?                     │ Solution = Top│
    │              │                          │ ranking member│
    │             No                          │    of P_t     │
    │              ▼                          └──────────────┘
    │    ┌─────────────────────┐
    │    │ Select the top elite members│
    │    │ for reproduction (E_t)│
    │    └─────────────────────┘
    │              │
    │              ▼
    │    ┌─────────────────────┐
    │    │ Crossover (weighted │
    │    │ average) of E_t members;│
    │    │ create offsprings (O_t)│
    │    └─────────────────────┘
    │              │
    │              ▼
    │    ┌─────────────────────┐
    │    │ Apply random mutations on│
    │    │ some of offsprings (O'_t)│
    │    └─────────────────────┘
    │              │
    │              ▼
    │    ┌─────────────────────┐
    │    │     t = t + 1       │
    │    │ (Next generation)   │
    │    └─────────────────────┘
    │              │
    │              ▼
    │    ┌─────────────────────┐
    └────│    P_t = O'_{t-1}   │
         │  (New population)   │
         └─────────────────────┘
```

Fig. 1. Flowchart of a General Implementation of Genetic Algorithm (GA).

4.1 Basic concepts

Particle swarm optimization (PSO) is a high-performance stochastical search algorithm that can also be used to solve inverse problems. The method is based on the social behavior of species in nature, e.g., a swarm of birds or a school of fish (Eberhart & Kennedy, 1995).

In the basic PSO algorithm, if a member of the swarm finds a desirable position, it will influence the traveling path of the rest of the swarm members. Every member searches in its vicinity, and not only learns from its own experience (obtained in the previous iterations),

but also benefits from the experiences of the other members of the swarm, especially from the experience of the best performer. The original PSO algorithm includes the following components (Clerc, 2006):

- *Particle Position Vector x*: For each particle, this vector stores its current location in the search domain. These are the values for which the value of the objective function is calculated, and the optimization problem is solved.
- *Particle Velocity Vector v*: For every particle, this vector determines the magnitude and direction of change in the position of that particle in the next iteration. This is the factor that causes the particles to move around the search space.
- *Best Solution of a Particle p*: For each particle, this is the position that has produced the lowest value of the objective function (the best solution with the lowest error in our case). So if *f* is the objective function that is supposed to be minimized; *i* is the index for each particle, and *m* is the iteration counter, then:

$$p_i^m = \underset{0 \le s \le m}{\arg\min}\left(f\left(x_i^s\right)\right) \tag{12}$$

- *Best Global Solution g*: This is the best single position found by all particles of the swarm, i.e., the single *p* point that produces the lowest value for the objective function, among all the swarm members. In other words, if *n* is the swarm size, then:

$$g^m = \underset{0 \le s \le m, 1 \le k \le n}{\arg\min}\left(f\left(x_k^s\right)\right) \tag{13}$$

The number of particles in the swarm (*n*) needs to be specified at the beginning. Fewer particles in the swarm results in lower computational effort in each iteration, but possibly higher number of iterations is required to find the global optimum. On the other hand, a larger population will have a higher computational expense in each iteration, but is expected to require less iterations to reach the global optimum point. Earlier studies have shown that a smaller population is normally preferred (Alrasheed et al., 2008; Karray & de Silva, 2004). This was also observed in our study; however, its effect seems to be insignificant.

The steps involved in the basic PSO algorithm are detailed below (Clerc, 2006):
1. Randomly initialize the positions and velocities for all of the particles in the swarm.
2. Evaluate the fitness of each swarm member (objective function value at each position point).
3. At iteration *m*, the velocity of the particle *i*, is updated as:

$$v_i^{m+1} = c_0 v_i^m + c_1 r_1 \left(p_i^m - x_i^m\right) + c_2 r_2 \left(g^m - x_i^m\right) \tag{14}$$

where x_i^m and v_i^m are the position and velocity of particle *i* at the *m*-th iteration, respectively; p_i^m and g^m are the best positions found up to now by this particle (local memory) and by the whole swarm (global memory) so far in the iterations, respectively; c_0 is called the inertia coefficient or the self-confidence parameter and is usually between zero and one; c_1 and c_2 are the acceleration coefficients that pull the particles toward the local and global best positions; and r_1 and r_2 are random vectors in the range of (0,1). The ratio between these

three parameters controls the effect of the previous velocities and the trade-off between the global and local exploration capabilities.

1. Update the position of each particle using the updated velocity and assuming unit time:

$$x_i^{m+1} = x_i^m + v_i^{m+1} \tag{15}$$

2. Repeat (2) – (4) until a convergence criterion (an acceptable fitness value or a certain maximum number of iterations) is satisfied.

There are some considerations that must be taken into account when updating velocity of particles (step 3 of the above algorithm). First, we need a value for the maximum velocity. A rule of thumb requires that, for a given dimension, the maximum velocity, $v_{i,\max}$, should be equal to one-half the range of possible values for the search space. For example, if the search space for a specific dimension is the interval [0, 100], we will take a maximum velocity of 50 for this dimension. If the velocity obtained from Equation (14) is higher than $v_{i,\max}$, then we will substitute the maximum velocity instead of v_i^{m+1}. The reason for having this maximum allowable velocity is to prevent the swarm from "*explosion*" (divergence). Another popular way of preventing divergence is a technique called "*constriction*", which dynamically scales the velocity update (Clerc, 2006). The first method was used in a previous research by the authors (Vakili & Gadala, 2009). However, further investigation showed that a better performance is obtained when combining the constriction technique with limiting the maximum velocity. In this chapter, the velocity updates are done using constriction and can be written as:

$$v_i^{m+1} = K \left(v_i^m + c_1 r_1 \left(p_i^m - x_i^m \right) + c_2 r_2 \left(g^m - x_i^m \right) \right) \tag{16}$$

where K is the constriction factor, and is calculated as (Clerc, 2006):

$$K = \frac{2}{\left| 2 - \varphi - \sqrt{\varphi^2 - 4\varphi} \right|} \tag{17}$$

where $\varphi = c_1 + c_2$. Here, following the recommendations in (Clerc, 2006), the initial values for c_1 and c_2 are set to 2.8 and 1.3, respectively. These values will be modified in subsequent iterations, as discussed below.

As mentioned above, the relation between the self-confidence parameter, c_0, and the acceleration coefficients, c_1 and c_2, determines the trade-off between the local and global search capabilities. When using the constriction concept, the constriction factor is responsible for this balance. As we progress in time through iterations, we get closer to the best value. Thus, a reduction in the value of the self-confidence parameter will limit the global exploration, and a more localized search will be performed. In this study, if the value of the best objective function is not changed in a certain number of iterations (10 iterations in our case), the value of K is multiplied by a number less than one (0.95 for our problems) to reduce it (i.e. $K^{new} = 0.95 K^{old}$). These numbers are mainly based on the authors' experience, and the performance is not very sensitive to their exact values. Some other researchers have used a linearly decreasing function to make the search more localized after the few initial

iterations (Alrasheed et al., 2008). These techniques are called "*dynamic adaptation*", and are very popular in the recent implementations of PSO (Fan & Chang, 2007).

Also, in updating the positions, one can impose a lower and an upper limit for the values, usually based on the physics of the problem. If the position values fall outside this range, several treatments are possible. In this study, we set the value to the limit that has been passed by the particle. Other ideas include substituting that particle with a randomly chosen other particle in the swarm, or penalizing this solution by increasing the value of the objective function.

Figure 2 shows a flowchart of the whole process. Figure 3 gives a visual representation of the basic velocity and position update equations.

4.2 Variations

Unfortunately, the basic PSO algorithm may get trapped in a local minimum, which can result in a slow convergence rate, or even premature convergence, especially for complex problems with many local optima. Therefore, several variants of PSO have been developed to improve the performance of the basic algorithm (Kennedy et al., 2001). Some variants try to add a chaotic acceleration factor to the position update equation, in order to prevent the algorithm from being trapped in local minima (Alrasheed et al., 2007). Others try to modify the velocity update equation to achieve this goal. One of these variants is called the Repulsive Particle Swarm Optimization (RPSO), and is based on the idea that repulsion between the particles can be effective in improving the global search capabilities and finding the global minimum (Urfalioglu, 2004; Lee et al., 2008). The velocity update equation for RPSO is

$$v_i^{m+1} = c_0 v_i^m + c_1 r_1 \left(p_i^m - x_i^m \right) + c_2 r_2 \left(p_j^m - x_i^m \right) + c_3 r_3 v_r \qquad (18)$$

where p_j^m is the best position of a randomly chosen other particle among the swarm, c_3 is an acceleration coefficient, r_3 is a random vector in the range of (0,1), and v_r is a random velocity component. Here c_2 is -1.43, and c_3 is 0.5. These values are based on recommendations in (Clerc, 2006). The newly introduced third term on the right-hand side of Eq. 18., with always a negative coefficient (c_2), causes a repulsion between the particle and the best position of a randomly chosen other particle. Its role is to prevent the population from being trapped in a local minimum. The fourth term generates noise in the particle's velocity in order to take the exploration to new areas in the search space.

Once again, we are gradually decreasing the weight of the self-confidence parameter. Note that the third term on the right-hand side of Eq. (1), i.e., the tendency toward the global best position, is not included in a repulsive particle swarm algorithm in most of the literature.

The repulsive particle swarm optimization technique does not benefit from the global best position found. A modification to RPSO that also uses the tendency towards the best global point is called the "Complete Repulsive Particle Swarm Optimization" or CRPSO (Vakili & Gadala, 2009). The velocity update equation for CPRSO will be:

$$v_i^{m+1} = c_0 v_i^m + c_1 r_1 \left(p_i^m - x_i^m \right) + c_2 r_2 \left(g^m - x_i^m \right) + c_3 r_3 \left(p_j^m - x_i^m \right) + c_4 r_4 v_r \qquad (19)$$

In CRPSO, by having both an attraction toward the particle's best performance, and a repulsion from the best performance of a random particle, we are trying to create a balance between the local and global search operations.
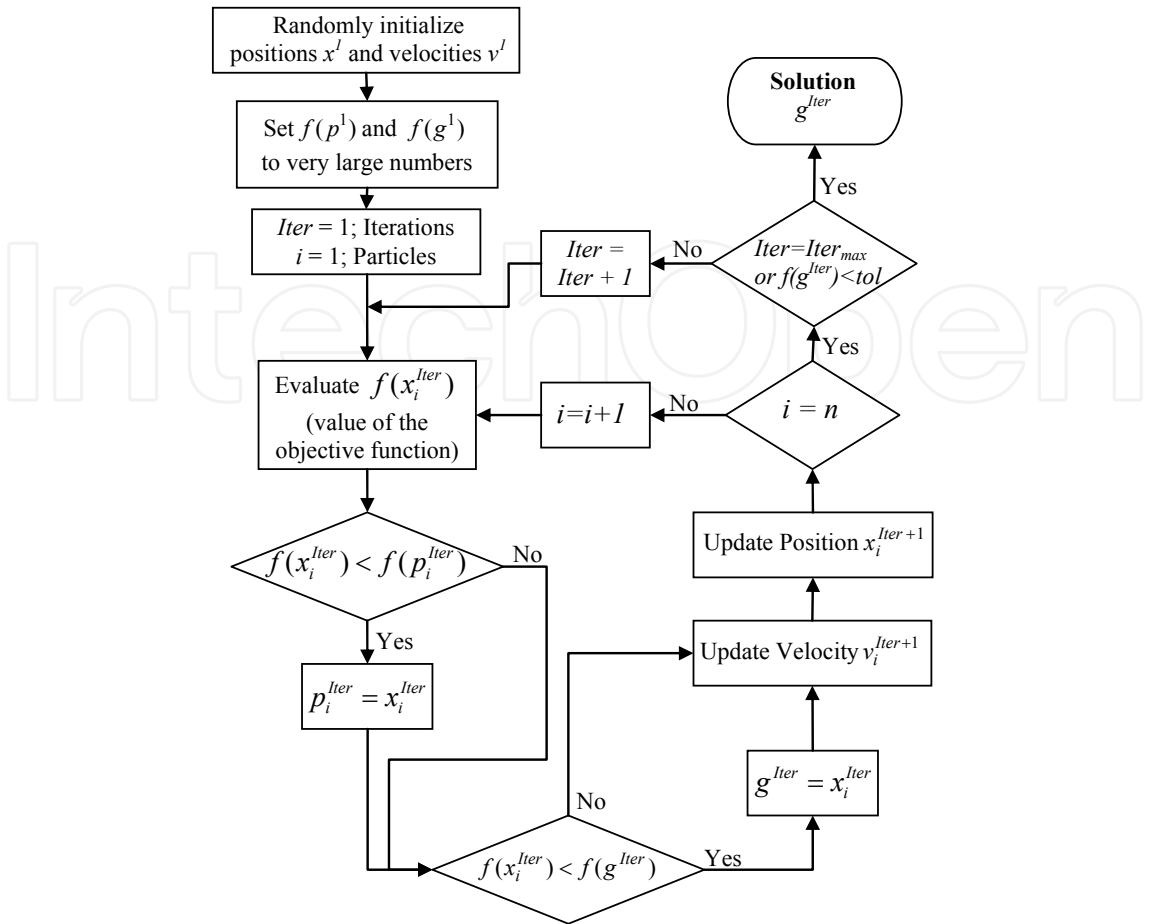
Fig. 2. Flowchart of the basic particle swarm optimization procedure.
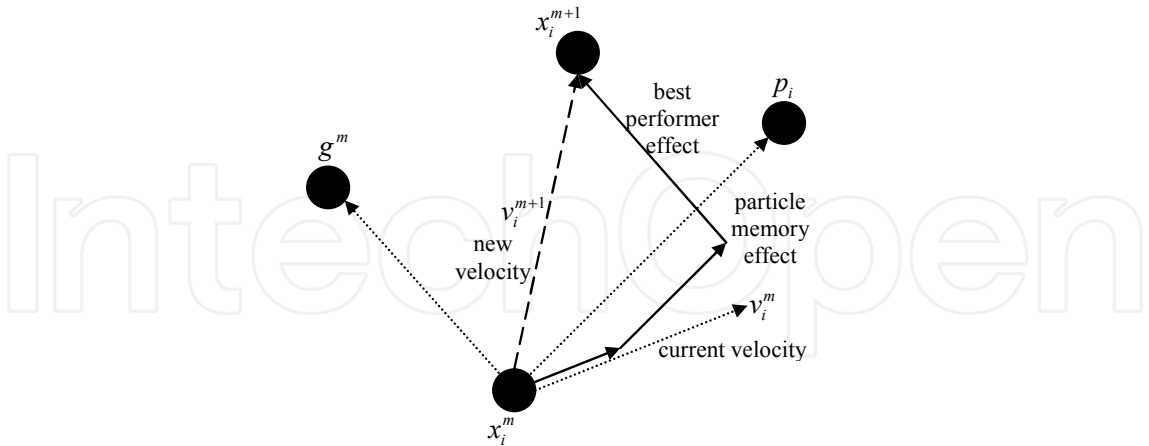

Fig. 3. Velocity and position updates in the basic particle swarm optimization algorithm.

Both RPSO and CRPSO were previously tested in solving inverse heat conduction problems by the authors (Vakili & Gadala, 2009). It was found that CRPSO shows better performance than the basic and repulsive PSO algorithms. In handling the noisy data, however, RPSO was the most efficient variation, followed closely by CRPSO. It was concluded then that the CRPSO variation is the suitable choice for IHCPs. Also, in (Vakili & Gadala, 2011), several

modifications were done on the formulation of inverse heat conduction problem as an optimization problem, as well as on the implementation of the PSO algorithm.

5. Artificial Neural Networks

Artificial Neural Networks (ANN) are motivated by the efficiency of brain in performing computations. These networks are made of a large number of processing units (neurons) that are interconnected through weighted connections, similar to synapses in brain. In order for the network to perform the expected tasks, it should first go through a "learning" process. There are two main categories of learning: supervised, or unsupervised. In supervised learning, the network learning is achieved by practicing on pre-designed training sets, while in unsupervised learning, the network is presented with a set of patterns, and learns to group these patterns into certain categories. The supervised learning is useful in function fitting and prediction, while unsupervised learning is more applicable to pattern recognition and data clustering. Since the learning process in our application is a supervised one, we focus on this type of learning process.

While there are several major classes of neural networks, in this chapter, we have studied only two of them, which are introduced in this section.

5.1 Feedforward Multilayer Perceptrons (FMLP)

In a feedforward network, the nodes are arranged in layers, starting from the input layer, and ending with the output layer. In between these two layers, a set of layers called hidden layers, are present, with the nodes in each layer connected to the ones in the next layer through some unidirectional paths. See Fig. 4 for a presentation of the topology. It is common to have different number of elements in the input and output vectors. These vectors can occur either concurrently (order is not important), or sequentially (order is important). In inverse heat conduction applications, normally the order of elements is important, so sequential vectors are used.
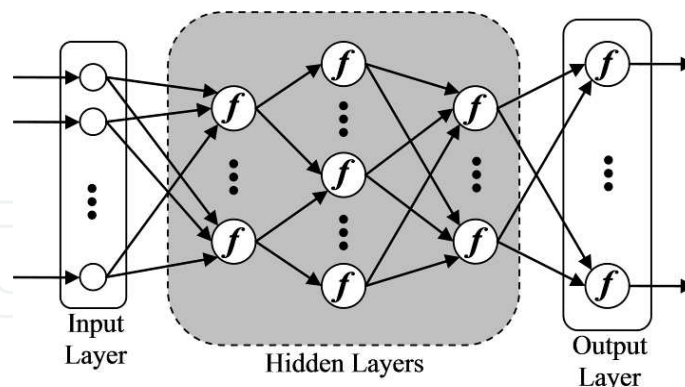

Fig. 4. A feedforward network topology.

5.2 Radial Basis Function Networks (RBFN)

The basic RBFN includes only an input layer, a single hidden layer, and an output layer. See Fig. 5 for a visual representation. The form of the radial basis function can be generally given by

$$f_i(\mathbf{x}) = r_i\left(\frac{\|\mathbf{x} - \mathbf{v}_i\|}{\sigma_i}\right) \tag{20}$$

in which $\mathbf{x}$ is the input vector, and $\mathbf{v}_i$ is the vector denoting the center of the receptive field unit f_i with σ_i as its unit width parameter. The most popular form of this function is the Gaussian kernel function, given as

$$f_i(\mathbf{x}) = \exp\left(\frac{-\|\mathbf{x} - \mathbf{v}_i\|^2}{2\sigma_i^2}\right) \tag{21}$$

These networks normally require more neurons than the feedforward networks, but they can be designed and trained much faster. However, in order to have a good performance, the training set should be available in the beginning of the process.
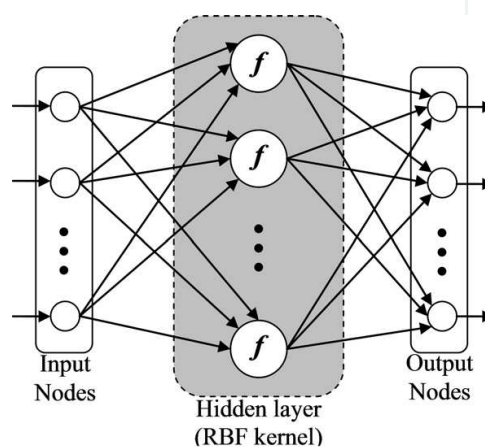
Fig. 5. An RBF network topology.

5.3 Implementation in inverse heat conduction problem

In order to use the artificial neural networks in the inverse heat conduction problem, we first started with a direct heat conduction finite element code, and applied several sets of heat fluxes in the boundary. The resulting temperatures in locations inside the domain, which correspond to the thermocouple locations in the experiments, were obtained. The neural network was then trained using the internal temperature history as an input, and the corresponding applied heat flux as the target. The assumption was that this way, the neural network should be able to act as an inverse analysis tool, and given a set of measured thermocouple readings, be able to reproduce the heat fluxes.

The obtained results, however, were far from satisfactory. It seemed that the relationship between the actual values of temperatures and heat fluxes is a complicated one, which is very hard for the neural networks to understand and simulate, at least when using a reasonably small number of layers. Thus, we decided to reformulate the problem, and use the change in the temperature in each time step as the input. In this formulation, neural networks performed much better, and a good quality was achieved in the solution in a reasonable amount of time.

Further investigations showed that if the time step size is varying, we can use a derivative of temperature with respect to the heat flux as the input, i.e. divide the temperature change by the time step size. The results were again satisfactory, however, more bookkeeping is needed, which complicates the implementation and makes the algorithm more prone to coding errors. This practice is not normally recommended, unless it can result in a considerable reduction in the solution time.

6. Test cases

A block containing nine thermocouples is modeled for each pass of water jet cooling of a steel strip. The length of the block is 114.3 mm (9 sections of each 12.7 mm). The width and thickness are 12.7 mm and 6.65 mm, respectively. To model the thermocouple hole, a cylinder of radius 0.5 mm and height of 5.65 mm is taken out of the block. Isoparametric eight-node brick elements are used to discretize the domain. Fig. 6(a) shows the whole domain, and Fig. 6(b) is a close-up view of one of the TC holes.

(a)   (b)
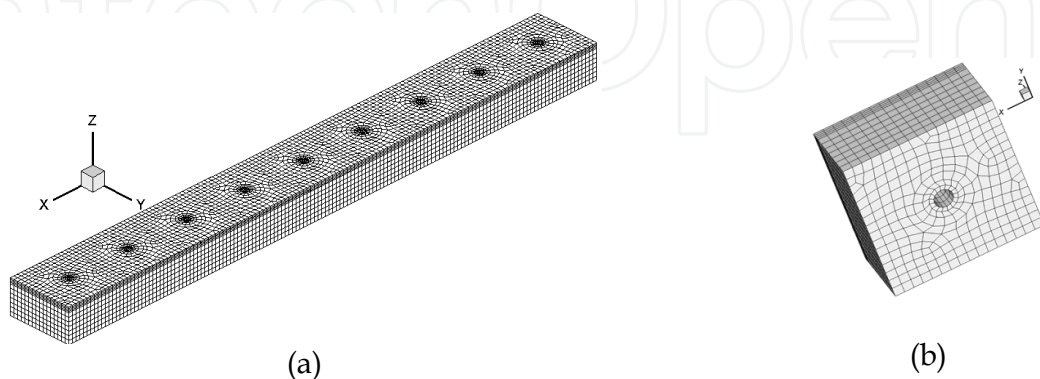
Fig. 6. (a) The whole block consisting of nine thermocouple zones; (b) A close-up view of the TC hole from bottom.

(a)   (b)
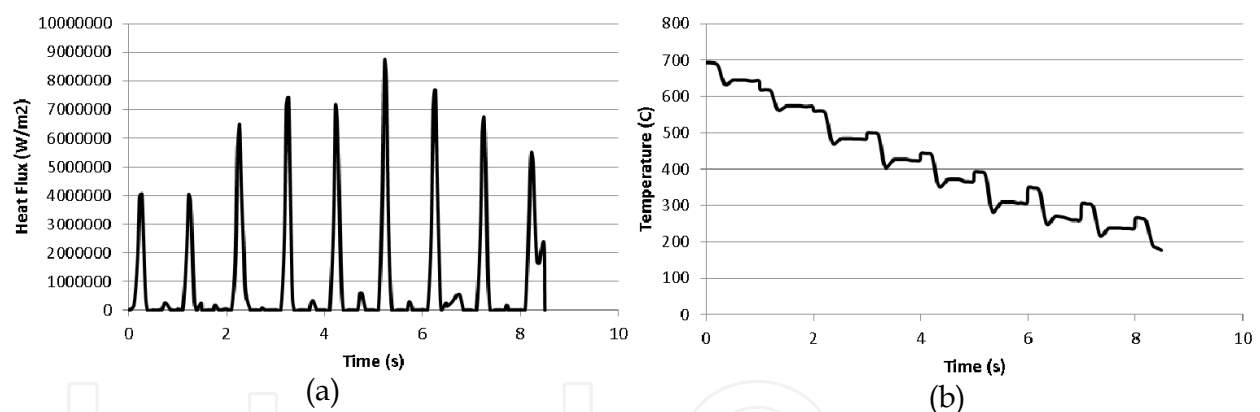
Fig. 7. Time history of cooling on a run-out table; (a) Surface heat fluxes; (b) Internal temperatures.

The boundary condition on the top surface is prescribed heat flux which is chosen to resemble the one in water cooling of steel strips. Figure 7(a) shows the applied heat fluxes on top of one of the thermocouple locations for the whole cooling process, while Figure 7(b) shows the history of the temperature drop at the corresponding thermocouple location. Figure 8(a) shows a close-up of the applied heat flux at five of the nine thermocouple locations. It is very similar to the actual heat flux values on a run-out table with two rows of staggered circular jets, impinging on the third and seventh locations (Vakili & Gadala, 2010). Figure 8(b) is a close-up view of the temperature history at five of the nine thermocouple locations inside the plate, obtained from direct finite element simulation. The other boundaries are assumed to be adiabatic. The density, ρ, is $7850 \, kg/m^3$, C_p is $475 \, J/kgK$, and the thermal conductivity, k, is first assumed to be constant and equal to $40 \, W/m.°C$ and later

changed to be depending on temperature, as will be discussed in section 7.4. These are the physical properties of the steel strips that are used in our controlled cooling experiment. Results are obtained at the top of the cylindrical hole, which is the assumed position of a thermocouple. Inverse analysis is conducted to obtain the transient heat flux profile at the top surface of the plate.
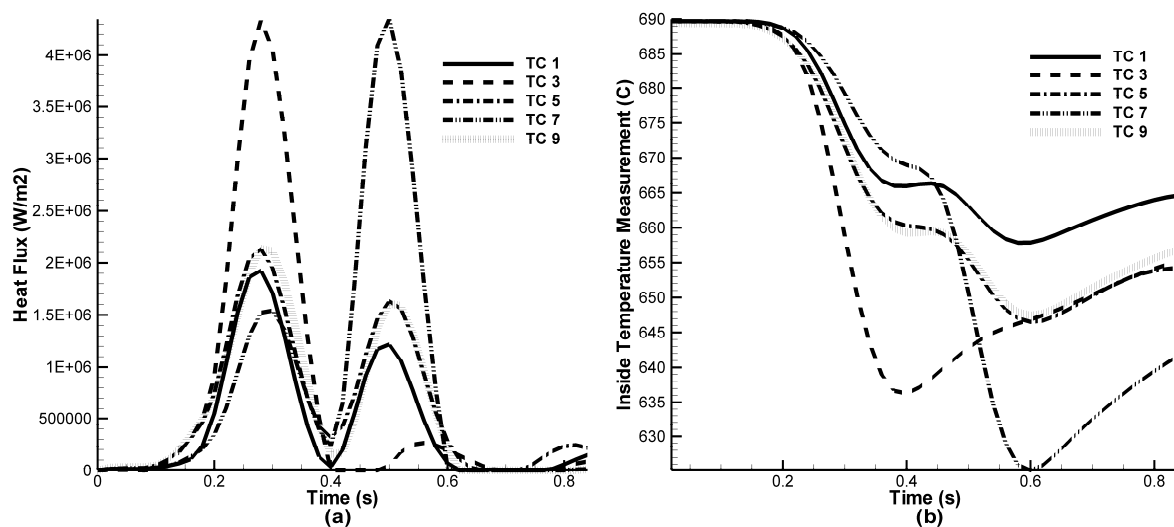

Fig. 8. (a) The applied heat flux on the top surface; (b) The thermocouple readings used for inverse analysis.

7. Results and discussion

As the first step in our study of these techniques, we investigate their capability in solving a general inverse heat conduction problem. We start by applying the artificial neural networks to the inverse heat conduction problem. This is different from GA and PSO, since those methods perform a stochastical search and are similar in many aspects, while the artificial neural networks are more like a correlation between the inputs and outputs. Fig. 9 shows the result of the application of the radial basis function neural networks for the whole history of the heat fluxes on the runout table. Temperatures start at 700 °C and go down to 176 °C. The heat flux vs. time profile is plotted in Fig. 9. As can be seen from this figure, neural networks are generally capable of dealing with the whole range of the cooling history.

However, this method has limitations, as observed in Fig. 9, and in more details in Fig. 10. The latter figure shows a close-up view of each of the 17 peaks of heat flux that happen during the cooling process on the run-out table, i.e. the peaks in Fig. 9. The circles are the expected heat flux, and the plusses are the result of NNs. The top left sub-figure is the first peak heat flux in time, and then it moves to the right, and then to the next row. Note that each even sub-figure (2nd, 4th, and so on) is a very smaller peak which is associated with the second row of jets. These peaks are not very obvious in Fig. 9, due to the scaling. Going through the subfigures of heat fluxes, it is apparent that the success or failure of NNs is not that much related to the temperature range, or the magnitude of heat fluxes, but on the actual shape of the heat flux profile. If the heat flux has a clear thin peak and two tails before and after the peak, the NN is doing a good job. However, the existence of other details in the

heat flux profile reduces the quality of the NN predictions. Also, considering the ill-posed nature of the problem, and all the complications that are involved, we can generally say that in most cases (about 75% of the cases) it does a decent job. Of course, there is the possibility of slightly improving the results by trying to modify the performance parameters of the NN, but overall we can say that NNs are more useful in getting a general picture of the solution, rather than producing a very accurate and detailed answer to the IHCP.

Fig. 9. Time History of Heat Fluxes in a Typical Run-Out Table Application; Expected Results (Squares) vs. the RBF Network Results (Line).

Fig. 10. Individual Heat Flux Peaks vs. Time from a Typical Run-Out Table Application; Expected Results (Circles) vs. the RBF Network Results (Pluses)

On the other hand, GA and PSO algorithms show reasonably good predictions of the details of the missing boundary conditions. Notice that we still need to have some form of regularization for these methods to work properly. The figures for the results of GA and PSO are not presented here for the sake of brevity, but can be found in (Vakili & Gadala, 2009). They will be used, however, for comparisons in the next sections.

7.1 Time step size
One of the main problems of the classical approaches, such as the sequential function specification method studied in this chapter, is their instability when small time steps are used. Unlike direct problems where the stability requirement gives the upper limit of the time step size, in inverse problems the time step is bounded from below. Fig. 11(a)(Vakili & Gadala, 2009) shows the oscillation in the results obtained by the function specification method and a time step size of 0.01 (s), which corresponds to the onset of instability. For time steps smaller than this, the whole process diverges. PSO, GA, and NNs successfully produce, however, the results for the same time step size as presented in Fig. 11(b) for PSO. Note that the oscillations here are not due to the instability caused by the time step size, and can be improved by performing more iterations. It is, however, important to mention that the time requirements for these techniques are much higher than those of the classical function specification approaches.

7.2 Efficiency
In this section, we compare the solution time required for GA, the three variations of PSO, and feed forward and radial basis function neural networks. We assume that there is no noise in the solution, and we compare the time that is required to get to certain accuracy in the heat flux predictions. Table 1 compares the solution time for different inverse analysis algorithms. The fastest solution technique is the gradient-based function specification method. The stochastical methods such as GA and PSO variants suffer a high computational cost. RBF neural networks perform much faster than GA and PSO, but they are still slower than the gradient-based methods, such as function specification.
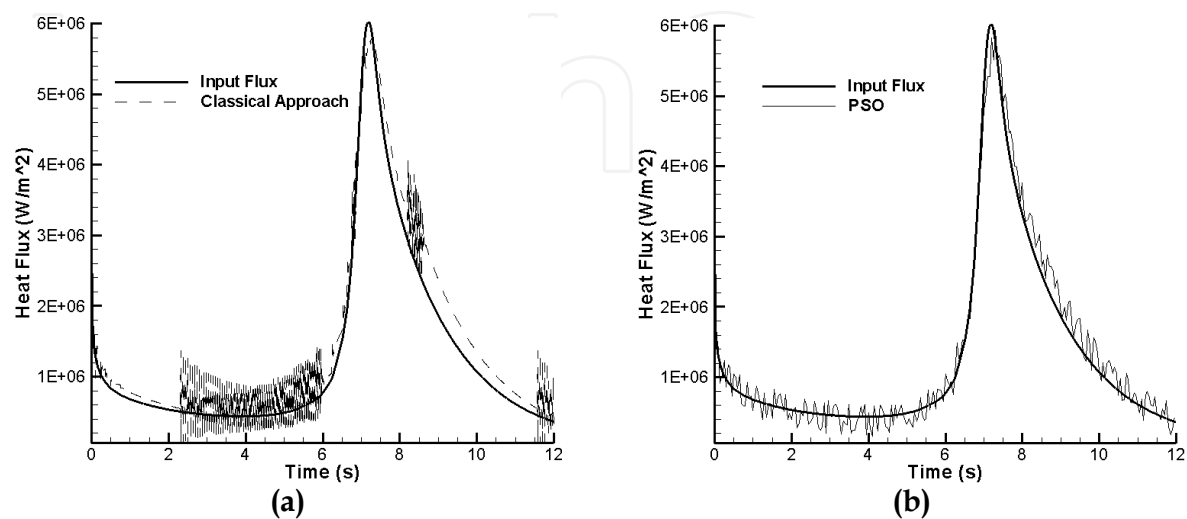

Fig. 11. Heat flux vs. time: (a) classical approach, (b) PSO (Vakili & Gadala, 2009).

Function Specification Method	GA	PSO	RPSO	CRPSO	FMLP	RBFN
Solution Time (s)	1406	8430	6189	5907	6136	7321	2316

Table 1. Comparison of the solution time for different inverse analysis algorithms.

A more detailed comparison between the efficiency of GA and PSO variations can be found in (Vakili & Gadala, 2009).

7.3 Noisy domain solution

To investigate the behavior of different inverse algorithm variations in dealing with noise in the data, a known boundary condition is first applied to the direct problem. The temperature at some internal point(s) will be calculated and stored. Then random errors are imposed onto the calculated exact internal temperatures with the following equation:

$$T_m = T_{exact} + \sigma \cdot r \tag{22}$$

where T_m is the virtual internal temperature that is used in the inverse calculations instead of the exact temperature, T_{exact}; r is a normally distributed random variable with zero mean and unit standard deviation; and σ is the standard deviation. Virtual errors of 0.1% and 1% of the temperature magnitude are investigated here.

We start by studying the effectiveness of the neural networks in handling noisy domains. Generally, the stability of the neural networks is on the same order as other inverse methods. It may be possible to tune the parameters to make it a little bit more stable, but generally it does not look promising in terms of noise resistance, since such modifications exist for almost all other methods. Fig. 12 - Fig. 13 show the results of the RBF network
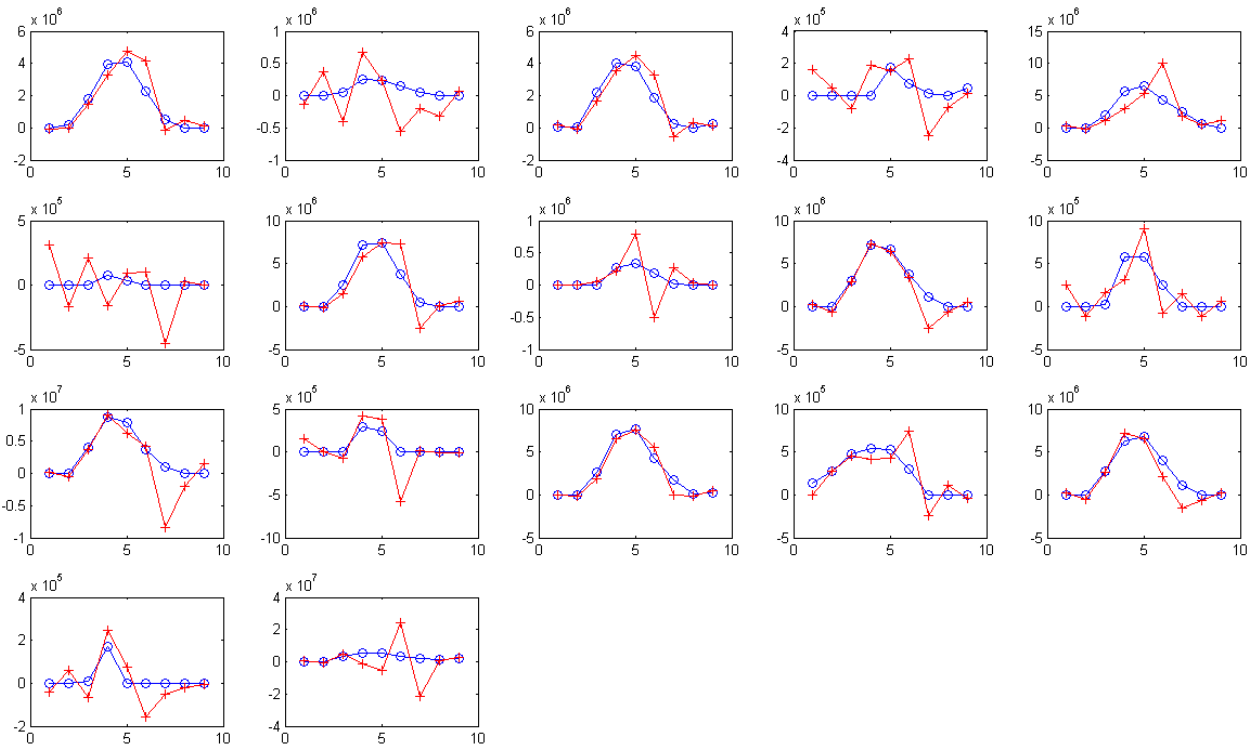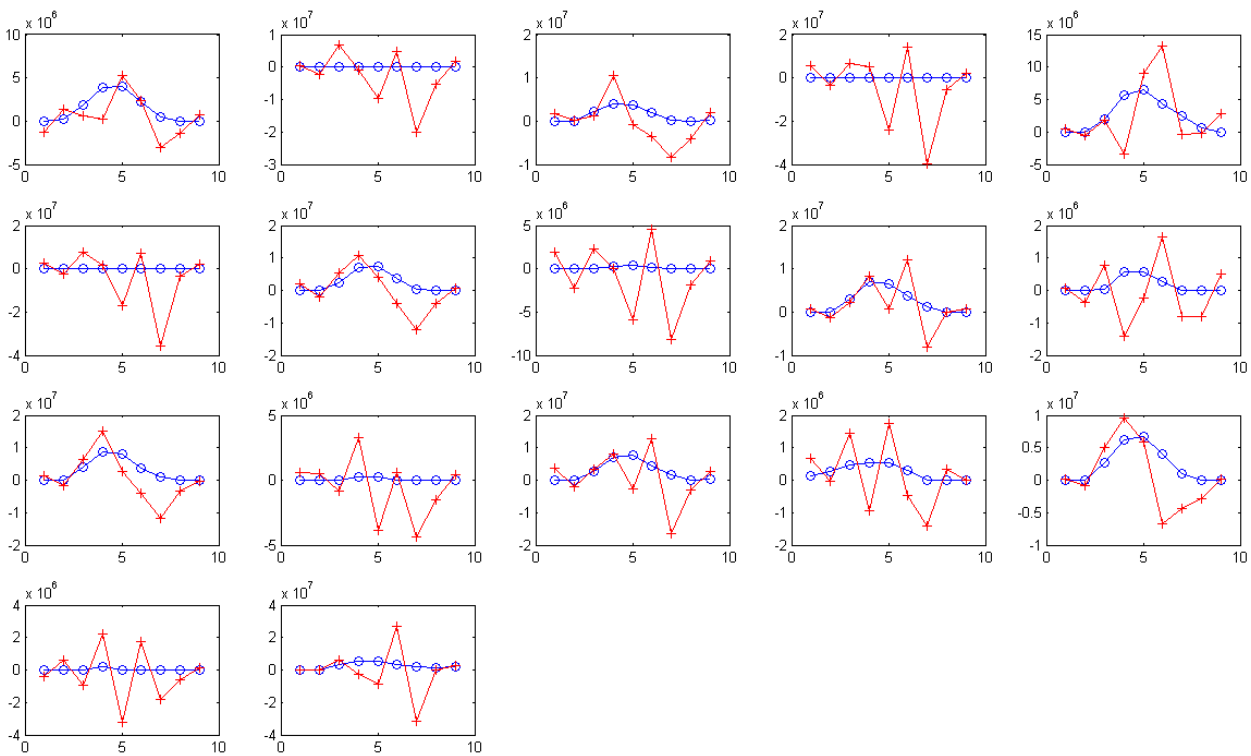

Fig. 12. Individual heat flux peaks vs. time from a typical run-out tale application; Expected results (blue circles) vs. the RBF network results (red pluses); Artificial noise added: c = ±0.1%.

(red pluses) versus the expected results (blue circles) for individual heat flux peaks during the cooling history of the plate. The amount of added noise in these figures is ±0.1%and ±1%, respectively.

There are several ways to make an inverse algorithm more stable when dealing with noisy data. For example, (Gadala & Xu, 2006) have shown that increasing the number of "*future time steps*" in their sequential function specification algorithm resulted in greater stability. They have also demonstrated that increasing the regularization parameter, *a*, improves the ability of the algorithm to handle noisy data. However, the latter approach was shown to greatly increase the required number of iterations, and in many cases the solution may diverge. In this work, we first examine the effect of the regularization parameter, and then investigate an approach unique to the PSO method, to improve the effectiveness of the inverse algorithm in dealing with noise.

Fig. 14 shows the effect of varying the regularization parameter value on the reconstructed heat flux, using the basic particle swarm optimization technique. Stable and accurate results are obtained for a range of values of $a = 10^{-12}$ to 10^{-10}. These results are very close to those reported in (Gadala & Xu, 2006), i.e., the proper values of *a* are very similar for the sequential specification approach and PSO.

Fig. 13. Individual heat flux peaks vs. time from a typical run-out tale application; Expected results (blue circles) vs. the RBF network results (red pluses); Artificial noise added: c = ±1%.

Another factor that can affect the performance of a PSO inverse approach in dealing with noisy data is the value of the self-confidence parameter, c_0, or the ratio between this parameter and the acceleration coefficients. The acceleration coefficients are set to the default value of 1.42. The initial value of the self-confidence parameter, c_0, is changed from the default value of 0.7. The results are shown below.
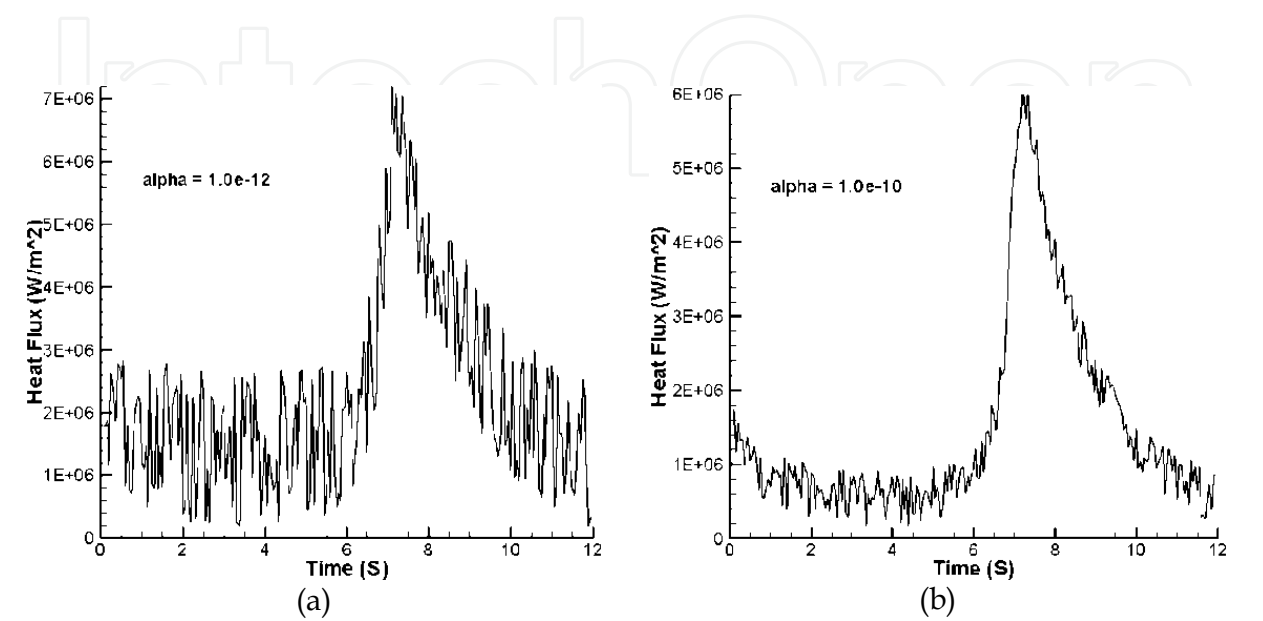

Fig. 14. Effect of Regularization Parameter; a: $\alpha = 10^{-12}$; b: $\alpha = 10^{-10}$
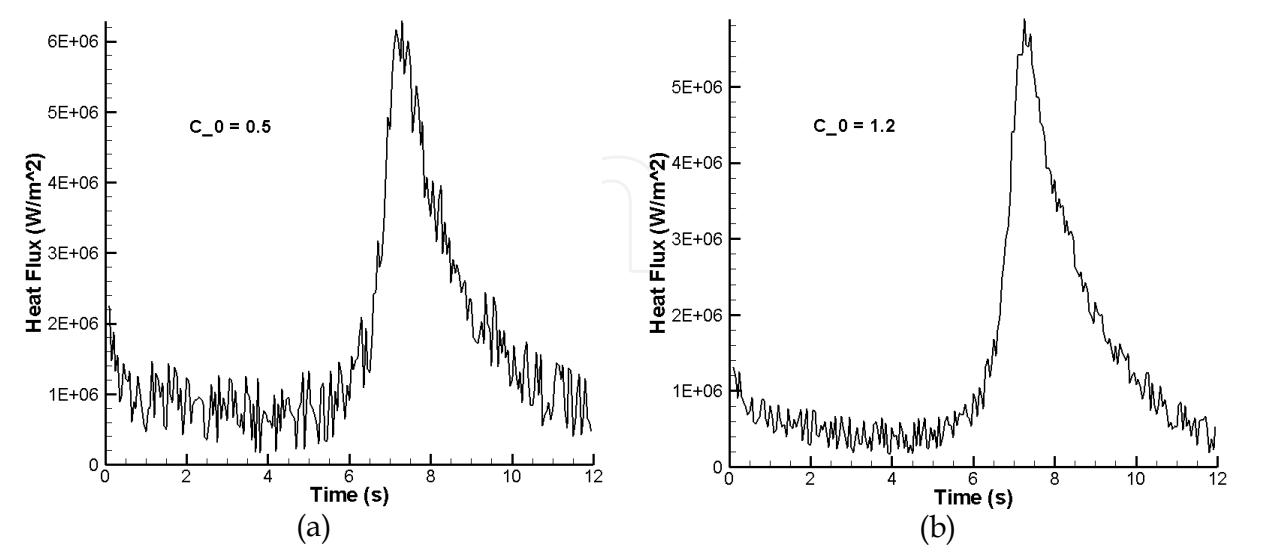
Fig. 15. Effect of Self-Confidence Parameter; (a) c0=0.5; (b) c0=1.2

As can be seen in Fig. 15 (for $a = 10^{-10}$), increasing the value of the self-confidence parameter results in better handling of the noisy data. This trend was observed for values up to approximately 1.3, after which the results become worse, and diverge. One possible explanation is that increasing the ratio of the self-confidence parameter with respect to the acceleration coefficients results in a more global search in the domain, and therefore increases the capability of the method to escape from the local minima caused by the noise, and find values closer to the global minimum. This effect was observed to be weaker in highly noisy domains. However, in the presence of a moderate amount of noise, increasing the self-confidence ratio results in more effectiveness. As can be seen in Table 2, the best effectiveness is normally obtained by RPSO, closely followed by CRPSO. Considering the higher efficiency of CRPSO, it is still recommended for the inverse heat conduction analysis.

C_0	0.7	0.8	0.95	1.1	1.2
PSO	8.105e+4	7.532e+4	7.079e+4	6.823e+4	6.257e+4
RPSO	7.577e+4	7.064e+4	6.685e+4	6.346e+4	5.816e+4
CRPSO	7.611e+4	6.739e+4	6.117e+4	5.999e+4	5.822e+4

Table 2. Effect of the Self-Confidence Parameter on the L2 Norm of Error in the Solution

Table 3 shows the value of L_2 norm of error in the solution, for ±1% added noise, and for different algorithms. It can be seen that the RBF neural networks perform better than the function specification method, and somewhere between the genetic algorithm and PSO variants. The most noise resistant algorithms are PSO variants, and the least stable algorithm is the gradient-based function specification method.

	Function Specification Method	GA	PSO	RPSO	CRPSO	FMLP	RBFN
L_2 Norm of Error	9.14e4		6.61e4	5.24e4	4.82e4	5.02e4	8.91e4	5.91e4

Table 3. The L2 Norm of Error in the Solution in a Noisy Domain for Different Algorithms

7.4 Effect of non-linearity

In many applications of inverse heat conduction, the thermophysical properties change with temperature. This results in nonlinearity of the problem. In other words, a same drop in the temperature values can be caused by different values of heat flux. So, a neural network that is trained with the relationship between the temperature change values and heat flux magnitudes may not be correctly capable of recognizing this nonlinear pattern, and as a result the performance will suffer. To investigate this effect, two kinds of expressions are used for thermal conductivity in this study. In one, we assume a constant thermal conductivity of W/m.°C, while in the other a temperature-dependent expression is used:

$$k = 60.571 - 0.03849 \times T \quad W/m.°C \qquad (23)$$

As expected, the nonlinearity will weaken the performance of both feedforward and radial basis function neural networks. The effect is seen as the training of the network stalls after a

number of epochs. In order to deal with this, increasing the number of hidden layers, increasing the number of neurons in each layer, and choosing different types of transfer function were investigated. However, none of these methods showed a significant improvement in the behavior of the network. The other methods of solving the inverse problem are much less sensitive to the effect of nonlinearity. Table 4 compares the error in the solution for both the linear and nonlinear cases, if the same numbers of iterations, generations, and epochs are used for different methods of solving the inverse heat conduction. As it can be seen, the neural networks methods perform very poorly in the nonlinear cases, while the other methods, either gradient based or stochastical, are immune to the problems caused by nonlinearity. Basically, neural networks, at least in the form that is used in this chapter, see nonlinearity as a kind of noise. It should be noted that neural networks can be useful in making rough estimates of the answer, or combined with some other techniques employed as an inverse solver for nonlinear cases (Aquino & Brigham, 2006), but on their own, are not a suitable choice for an accurate prediction of the boundary conditions in a nonlinear inverse heat conduction problem.

	Function Specification Method	GA	PSO	RPSO	CRPSO	FMLP	RBFN
Linear	1.81e2	7.62e2	3.85e2	3.42e2	3.17e2	9.90e2	5.35e2
Nonlinear	2.14e2	7.71e2	4.46e2	5.12e2	4.26e2	3.57e4	2.76e4

Table 4. The L_2 norm of error in the solution in an exact domain for different algorithms.

8. Conclusion

In this chapter, we introduced a gradient-based inverse solver to obtain the missing boundary conditions based on the readings of internal thermocouples. The results show that the method is very sensitive to measurement errors, and becomes unstable when small time steps are used. Then, we tried to find algorithms that are capable of solving the inverse heat conduction problem without the shortcomings of the gradient-based methods.

The artificial neural networks are capable of capturing the whole thermal history on the run-out table, but are not very effective in restoring the detailed behavior of the boundary conditions. Also, they behave poorly in nonlinear cases and where the boundary condition profile is different.

GA and PSO are more effective in finding a detailed representation of the time-varying boundary conditions, as well as in nonlinear cases. However, their convergence takes longer. A variation of the basic PSO, called CRPSO, showed the best performance among the three versions. The effectiveness of PSO was also studied in the presence of noise. PSO proved to be effective in handling noisy data, especially when its performance parameters were tuned. The proper choice of the regularization parameter helped PSO deal with noisy data, similar to the way it helps the classical function specification approaches. An increase in the self-confidence parameter was also found to be effective, as it increased the global search capabilities of the algorithm. RPSO was the most effective variation in dealing with noise, closely followed by CRPSO. The latter variation is recommended for inverse heat conduction problems, as it combines the efficiency and effectiveness required by these problems.

9. References

Abou khachfe, R., and Jarny, Y. (2001). Determination of Heat Sources and Heat Transfer Coefficient for Two-Dimensional Heat flow–numerical and Experimental Study. *International Journal of Heat and Mass Transfer*, Vol. 44, No. 7 , pp.1309-1322.

Alifanov, O. M., Nenarokomov, A. V., Budnik, S. A., Michailov, V. V., and Ydin, V. M. (2004). Identification of Thermal Properties of Materials with Applications for Spacecraft Structures. *Inverse Problems in Science and Engineering*, Vol. 12, No. 5 , pp.579-594.

Alifanov, O.M., (1995). *Inverse Heat Transfer Problems,* Berlin ; New York: Springer-Verlag.

Al-Khalidy, N., (1998). A General Space Marching Algorithm for the Solution of Two-Dimensional Boundary Inverse Heat Conduction Problems. *Numerical Heat Transfer, Part B*, Vol. 34, , pp.339-360.

Alrasheed, M.R., de Silva, C.W., and Gadala, M.S. (2008).Evolutionary Optimization in the Design of a Heat Sink, in: *Mechatronic Systems: Devices, Design, Control, Operation and Monitoring,* C. W. de Silva, Taylor & Francis.

Alrasheed, M.R., de Silva, C.W., and Gadala, M.S. (2007).A Modified Particle Swarm Optimization Scheme and its Application in Electronic Heat Sink Design, ASME/Pacific Rim Technical Conference and Exhibition on Packaging and Integration of Electronic and Photonic Systems, MEMS, and NEMS.

Aquino, W., and Brigham, J. C. (2006). Self-Learning Finite Elements for Inverse Estimation of Thermal Constitutive Models. *International Journal of Heat and Mass Transfer*, Vol. 49, No. 15-16 , pp.2466-2478.

Bass, B. R., (1980). Application of the Finite Element Method to the Nonlinear Inverse Heat Conduction Problem using Beck's Second Method. *Journal of Engineering and Industry*, Vol. 102, , pp.168-176.

Battaglia, J. L., (2002). A Modal Approach to Solve Inverse Heat Conduction Problems. *Inverse Problems in Engineering*, Vol. 10, No. 1 , pp.41-63.

Beck, J. V., Blackwell, B., and Haji-Sheikh, A. (1996). Comparison of some Inverse Heat Conduction Methods using Experimental Data. *International Journal of Heat and Mass Transfer*, Vol. 39, , pp.3649-3657.

Beck, J. V., and Murio, D. A. (1986). Combined Function Specification-Regularization Procedure for Solution of Inverse Heat Conduction Problem. *AIAA Journal*, Vol. 24, No. 1 , pp.180-185.

Beck, J.V., Blackwell, B., and Clair Jr, C.R.S. (1985). *Inverse Heat Conduction: Ill-Posed Problem,* New York: Wiley-Interscience Publication.

Beck, J.V., and Arnold, K.J. (1977). *Parameter Estimation in Engineering and Science,* New York: Wiley.

Blanc, G., Raynaud, M., and Chau, T. H. (1998). A Guide for the use of the Function Specification Method for 2D Inverse Heat Conduction Problems. *Revue Generale De Thermique*, Vol. 37, No. 1 , pp.17-30.

Clerc, M., (2006). *Particle Swarm Optimization,* ISTE.

Davis, L., (1991). *Handbook of Genetic Algorithms,* Thomson Publishing Group.

Eberhart, R., and Kennedy, J. (1995).A New Optimizer using Particle Swarm Theory, Proceedings of the Sixth International Symposium on Micro Machine and Human Science pp. 39-43.

Fan, S.K.S., and Chang, J.M. (2007).A Modified Particle Swarm Optimizer using an Adaptive Dynamic Weight Scheme, in: *Digital Human Modeling,* V. G. Duffy, Springer Berlin / Heidelberg. pp. 56-65, .

Gadala, M. S., and Xu, F. (2006). An FE-Based Sequential Inverse Algorithm for Heat Flux Calculation during Impingement Water Cooling. *International Journal of Numerical Methods for Heat and Fluid Flow*, Vol. 16, No. 3 , pp.356-385.

Girault, M., Petit, D., and Videcoq, E. (2003). The use of Model Reduction and Function Decomposition for Identifying Boundary Conditions of A Linear Thermal System. *Inverse Problems in Science and Engineering*, Vol. 11, No. 5 , pp.425-455.

Goldberg, D.E., (1989). *Genetic Algorithms in Search, Optimization and Machine Learning,* Addison-Wesley Longman Publishing Co., Inc. Boston, MA, USA.

Gosselin, L., Tye-Gingras, M., and Mathieu-Potvin, F. (2009). Review of Utilization of Genetic Algorithms in Heat Transfer Problems. *International Journal of Heat and Mass Transfer*, Vol. 52, No. 9-10 , pp.2169-2188.

Hassan, R., Cohanim, B., de Weck, O., and Venter, G. (2005).A Comparison of Particle Swarm Optimization and the Genetic Algorithm, Proceedings of the 46th AIAA/ASME/ASCE/AHS/ASC Structures, Structural Dynamics and Materials Conference.

Huang, C. H., Yuan, I. C., and Herchang, A. (2003). A Three-Dimensional Inverse Problem in Imaging the Local Heat Transfer Coefficients for Plate Finned-Tube Heat Exchangers. *International Journal of Heat and Mass Transfer*, Vol. 46, No. 19 , pp.3629-3638.

Huang, C. H., and Wang, S. P. (1999). A Three-Dimensional Inverse Heat Conduction Problem in Estimating Surface Heat Flux by Conjugate Gradient Method. *International Journal of Heat and Mass Transfer*, Vol. 42, No. 18 , pp.3387-3403.

Karr, C. L., Yakushin, I., and Nicolosi, K. (2000). Solving Inverse Initial-Value, Boundary-Value Problems Via Genetic Algorithm. *Engineering Applications of Artificial Intelligence*, Vol. 13, No. 6 , pp.625-633.

Karray, F.O., and de Silva, C.W. (2004). *Soft Computing and Intelligent System Design - Theory, Tools, and Applications,* New York: Addison Wesley.

Kennedy, J., Eberhart, R.C., and Shi, Y. (2001). *Swarm Intelligence,* Morgan Kaufmann.

Kim, H. K., and Oh, S. I. (2001). Evaluation of Heat Transfer Coefficient during Heat Treatment by Inverse Analysis. *Journal of Material Processing Technology*, Vol. 112, , pp.157-165.

Kim, S. K., and Lee, W. I. (2002). Solution of Inverse Heat Conduction Problems using Maximum Entropy Method. *International Journal of Heat and Mass Transfer*, Vol. 45, No. 2 , pp.381-391.

Krejsa, J., Woodbury, K. A., Ratliff, J. D., and Raudensky, M. (1999). Assessment of Strategies and Potential for Neural Networks in the IHCP. *Inverse Problems in Engineering*, Vol. 7, No. 3 , pp.197-213.

Kumagai, S., Suzuki, S., Sano, Y.R., and Kawazoe, M. (1995).Transient Cooling of Hot Slab by an Impinging Jet with Boiling Heat Transfer, ASME/JSME Thermal Engineering Conference pp. 347-352.

Lecoeuche, S., Mercere, G., and Lalot, S. (2006). Evaluating Time-Dependent Heat Fluxes using Artificial Neural Networks. *Inverse Problems in Science and Engineering*, Vol. 14, No. 2 , pp.97-109.

Lee, K. H., Baek, S. W., and Kim, K. W. (2008). Inverse Radiation Analysis using Repulsive Particle Swarm Optimization Algorithm. *International Journal of Heat and Mass Transfer*, Vol. 51, , pp.2772-2783.

Louahia-Gualous, H., Panday, P. K., and Artioukhine, E. A. (2003). Inverse Determination of the Local Heat Transfer Coefficients for Nucleate Boiling on a Horizontal Pipe Cylinder. *Journal of Heat Transfer*, Vol. 125, , pp.1087-1095.

Osman, A. S., (1190). Investigation of Transient Heat Transfer Coefficients in Quenching Experiments. *Journal of Heat Transfer*, Vol. 112, , pp.843-848.

Ostrowski, Z., R. A. Bialstrokecki, and A. J. Kassab. "Solving Inverse Heat Conduction Problems using Trained POD-RBF Network Inverse Method." *Inverse Problems in Science and Engineering* (2007).

Ozisik, M.N., (2000). *Inverse Heat Transfer: Fundamentals and Applications,* New York: Taylor & Francis.

Pietrzyk, M., and Lenard, J. G. (1990). A Study of Heat Transfer during Flat Rolling. *International Journal of Numerical Methods in Engineering*, Vol. 30, , pp.1459-1469.

Raudensky, M., Woodbury, K. A., Kral, J., and Brezina, T. (1995). Genetic Algorithm in Solution of Inverse Heat Conduction Problems. *Numerical Heat Transfer, Part B: Fundamentals*, Vol. 28, No. 3 , pp.293-306.

Roudbari, S., (2006). Self Adaptive Finite Element Analysis, Cornell University, .

Shiguemori, E. H., Da Silva, J. D. S., and De Campos Velho, H. F. (2004). Estmiation of Initial Condition in Heat Conduction by Neural Networks. *Inverse Problems in Science and Engineering*, Vol. 12, No. 3 , pp.317-328.

Silieti, M., Divo, E., and Kassab, A. J. (2005). An Inverse Boundary Element method/genetic Algorithm Based Approach for Retrieval of Multi-Dimensional Heat Transfer Coefficients within Film Cooling holes/slots. *Inverse Problems in Science and Engineering*, Vol. 13, No. 1 , pp.79-98.

Urfalioglu, O., (2004).Robust Estimation of Camera Rotation, Translation and Focal Length at High Outlier Rates, The First Canadian Conference on Computer and Robot Vision pp. 464-471.

Vakili, S., and Gadala, M. S. (2011). A Modified Sequential Particle Swarm Optimization Algorithm with Future Time Data for Solving Transient Inverse Heat Conduction Problems. *Numerical Heat Transfer, Part A: Applications*, Vol. 59, No. 12 , pp.911-933.

Vakili, S., and Gadala, M. S. (2010). Boiling Heat Transfer of Multiple Impinging Round Jets on a Hot Moving Plate. *Submitted to Heat Transfer Engineering* .

Vakili, S., and Gadala, M. S. (2009). Effectiveness and Efficiency of Particle Swarm Optimization Technique in Inverse Heat Conduction Analysis. *Numerical Heat Transfer, Part B: Fundamentals*, Vol. 56, No. 2 , pp.119-141.

Woodbury, K. A., and Thakur, S. K. (1996). Redundant Data and Future Times in the Inverse Heat Conduction Problem. *Inverse Problems in Science and Engineering*, Vol. 2, No. 4 , pp.319-333.

Heat Conduction - Basic Research

Edited by Prof. Vyacheslav Vikhrenko

The content of this book covers several up-to-date approaches in the heat conduction theory such as inverse heat conduction problems, non-linear and non-classic heat conduction equations, coupled thermal and electromagnetic or mechanical effects and numerical methods for solving heat conduction equations as well. The book is comprised of 14 chapters divided into four sections. In the first section inverse heat conduction problems are discuss. The first two chapters of the second section are devoted to construction of analytical solutions of nonlinear heat conduction problems. In the last two chapters of this section wavelike solutions are attained.The third section is devoted to combined effects of heat conduction and electromagnetic interactions in plasmas or in pyroelectric material elastic deformations and hydrodynamics. Two chapters in the last section are dedicated to numerical methods for solving heat conduction problems.

How to reference

In order to correctly reference this scholarly work, feel free to copy and paste the following:

M. S. Gadala and S. Vakili (2011). Assessment of Various Methods in Solving Inverse Heat Conduction Problems, Heat Conduction - Basic Research, Prof. Vyacheslav Vikhrenko (Ed.), ISBN: 978-953-307-404-7, InTech, Available from: http://www.intechopen.com/books/heat-conduction-basic-research/assessment-of-various-methods-in-solving-inverse-heat-conduction-problems

INTECH

open science | open minds